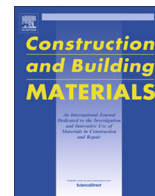




Contents lists available at ScienceDirect

# Construction and Building Materials

journal homepage: [www.elsevier.com/locate/conbuildmat](http://www.elsevier.com/locate/conbuildmat)

## Masonry mortars, precast concrete and masonry units using coal bottom ash as a partial replacement for conventional aggregates



Roberto Rodríguez-Álvarez, Belén González-Fonteboa\*, Sindy Seara-Paz, Emilio José Rey-Bouzón

Department of Civil Engineering, Campus de Elviña s/n, 15071 A Coruña, Universidade da Coruña, Spain

### HIGHLIGHTS

- Coal bottom ash (CBA) is a waste that is produced worldwide in large amounts.
- Scientific literature on masonry mortars and precast concrete using CBA is scarce.
- CBA particles are irregular in shape, rough in texture, light and highly absorbent.
- A high CBA content negatively affects workability, strength and durability.
- CBA2 is proposed as a possible internal curing water reservoir.

### ARTICLE INFO

#### Article history:

Received 3 November 2020

Received in revised form 12 January 2021

Accepted 15 February 2021

Available online 27 February 2021

#### Keywords:

Cement based material

Joint

Plaster

Render

Coating

Prefabricated

Blocks

Coal combustion products

Waste

Residues

### ABSTRACT

Granular coal combustion products are problematic waste materials whose use as aggregates in concrete has been extensively studied. However, its integration into other non-structural materials and elements has not been so widely documented. Masonry mortars, precast concrete and masonry units with different ratios of coal bottom ash replacing conventional aggregates have been studied. With the incorporation of coal bottom ash in the mortars, the workability, density and strength decrease whereas the porosity, the weight loss and the drying shrinkage increase. However, low replacement ratios have slight effects. The use of coal bottom ash as an internal curing water reservoir is proposed as the most promising future line of research.

© 2021 The Authors. Published by Elsevier Ltd. This is an open access article under the CC BY-NC-ND license (<http://creativecommons.org/licenses/by-nc-nd/4.0/>).

### 1. Introduction

Climate change and other environmental concerns have promoted the growth of renewable energies throughout the world. However, coal is still an important energy source, especially for electricity generation. The proportion of this fuel in the energy mix varies broadly between different regions. For instance, some European countries still use coal as their principal source of energy, whereas some others are remarkably reducing their coal depen-

dence (Fig. 1). For example, Spain registered their first days with no coal consumption in December 2019 [1].

Coal combustion generates large amounts of different waste such as fly ash, bottom ash (CBA), boiler slag and flue gas desulfurization sub-products. Successful experiences regarding their integration into some construction materials have been reported despite some challenges. For example, some coal properties are critically influenced by its source, which can vary between plants located in the same country or even over time in the same plant. This happens because many countries supply their power stations with imported coal (Fig. 2).

The scope of this work is limited to coal combustion waste material which is granular in nature. This is mainly CBA and boiler slag and will be referred to as granular coal combustion products (GCCP). Many scientific works have addressed the use of GCCP in concrete and some have collated the obtained results [3–8]. They

\* Corresponding author.

E-mail addresses: [roberto.rodriguez1@udc.es](mailto:roberto.rodriguez1@udc.es) (R. Rodríguez-Álvarez), [bfonteboa@udc.es](mailto:bfonteboa@udc.es) (B. González-Fonteboa), [gumersinda.spaz@udc.es](mailto:gumersinda.spaz@udc.es) (S. Seara-Paz), [emilio.rey.bouzón@udc.es](mailto:emilio.rey.bouzón@udc.es) (E.J. Rey-Bouzón).

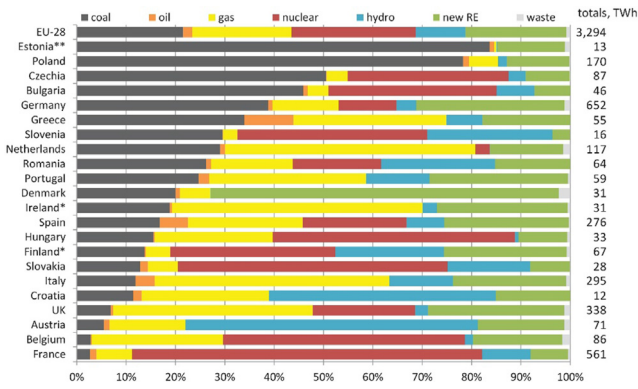


Fig. 1. Energy mix for EU electricity generation in 2017 [2].

conclude that the use of GCCP increases the porosity of concrete [9–13], decreases its strength [14–19], increases its water absorption capacity [20–25] and jeopardizes other durability properties [26–30]. However, the integration of this by-product into other materials such as roller compacted concrete [31,32], pervious concrete [33–35], paving blocks [36–38], masonry units [39–41], masonry mortars [42–44], grouts [45] and other non-structural materials [46–50] has not been so extensively studied. Furthermore, some of the least scientifically documented materials have been successfully integrated into GCCP for decades. Some examples of this are asphalt mixtures and granular road bases [51]. Also, several patents regarding the use of GCCP as an aggregate have been developed in the USA [52]. In the past, financial savings were the main motivation for the use of GCCP in construction materials [52]. Nowadays, environmental concerns are firmly encouraging its promotion. Furthermore, some research works have proven that the use of GCCP as aggregate can significantly decrease the density of concrete [9–13,18,22,24,26,28,53–55] leading to easier handling and a decrease in thermal conductivity (Fig. 3 a & b).

These two effects of GCCP are especially beneficial in some building elements such as masonry units (concrete blocks) and coatings whose capacity to integrate alternative aggregates has been recognized [56–62]. Masonry units with GCCP, known as cinder blocks, have been successfully manufactured since the beginning of the 20th century [63]. Actually, the ASTM C331-17 [64] standard specifies the requirements for GCCP to be used in such application. However, masonry mortars with GCCP are not popular for use in the field.

The objective of this study is to provide some experimental results for the use of CBA in masonry mortars, precast concrete and masonry units, and therefore contribute to filling in the gap in the scientific knowledge regarding the integration of this by-product into these construction materials. Conclusions have been made about the effect of the partial replacement of conventional aggregate with CBA and future lines of research are proposed.

## 2. Materials characterization

The two different CBAs used in this study are named CBA1 and CBA2. They are produced in the combustion of Russian bituminous coal and Indonesian subbituminous coal, respectively. In both cases, the coal is pulverized before combustion, no specific measures are taken to minimize sulphur-rich emissions and the boiler emptying process is wet. Both ashes are aggregate-like in appearance (Fig. 4 a,f), irregular in shape with some elongated particles (Fig. 4 b,c,d,g,h,i) and porous in texture (Fig. 4 e,j). Spherical particles are observed among the smallest sizes of CBA1 (Fig. 4 d) while the texture of CBA2 is more variable (Fig. 4 j).

Thermogravimetric analysis (TGA) of CBA1 and CBA2 is carried out and the weight loss curves of the two waste materials are depicted in Fig. 5. Most of the weight loss is related to the presence of unburnt coal in both CBA1 and CBA2. Differences in the position of the maximum weight loss rate and the intensity of the weight loss (3.9% for CBA1 and 27.1% for CBA2) are related to the nature of the coal and the ash generation and collection processes followed at the power stations.

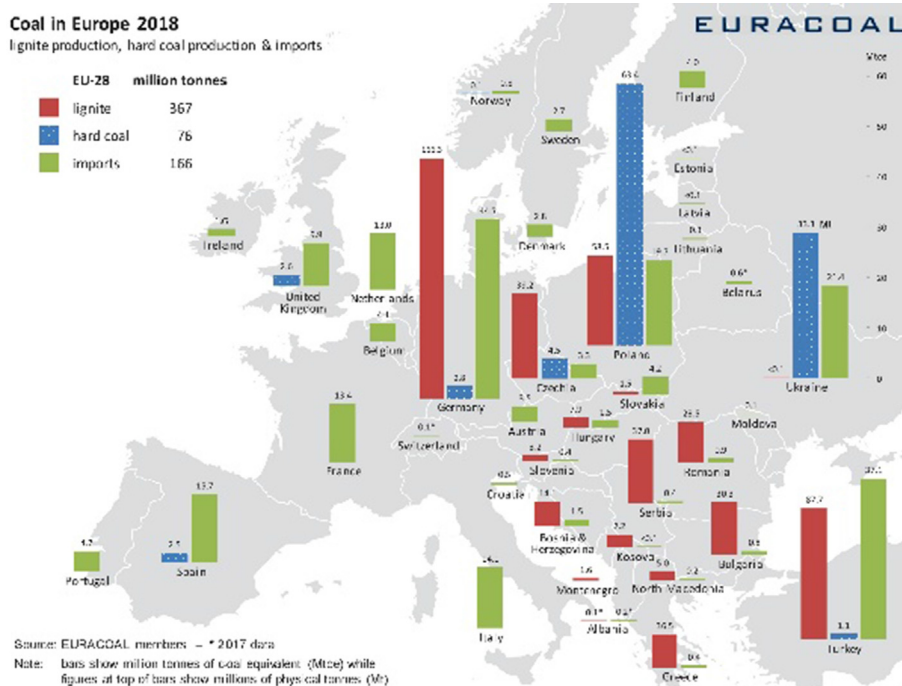


Fig. 2. Coal in Europe, 2018: Lignite production, hard coal production and imports [2].

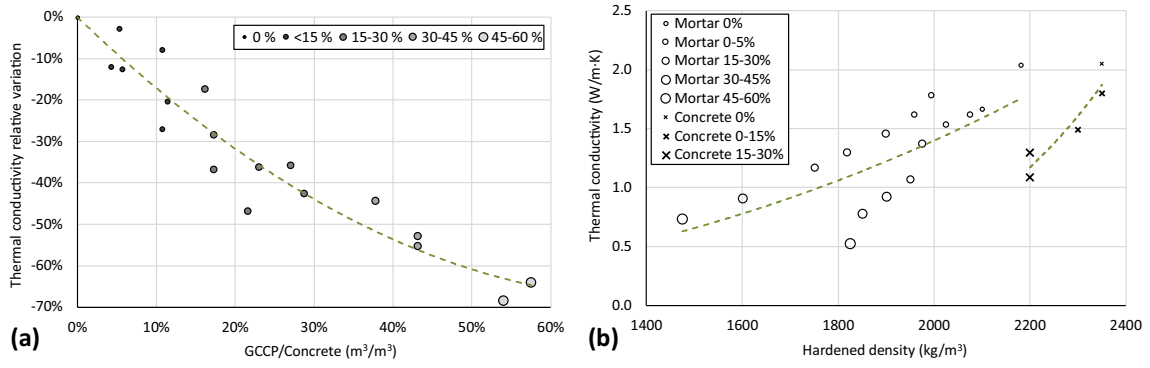


Fig. 3. (a) Thermal conductivity relative variation and (b) relationship between thermal conductivity and hardened density for different GCCP content [9,10].

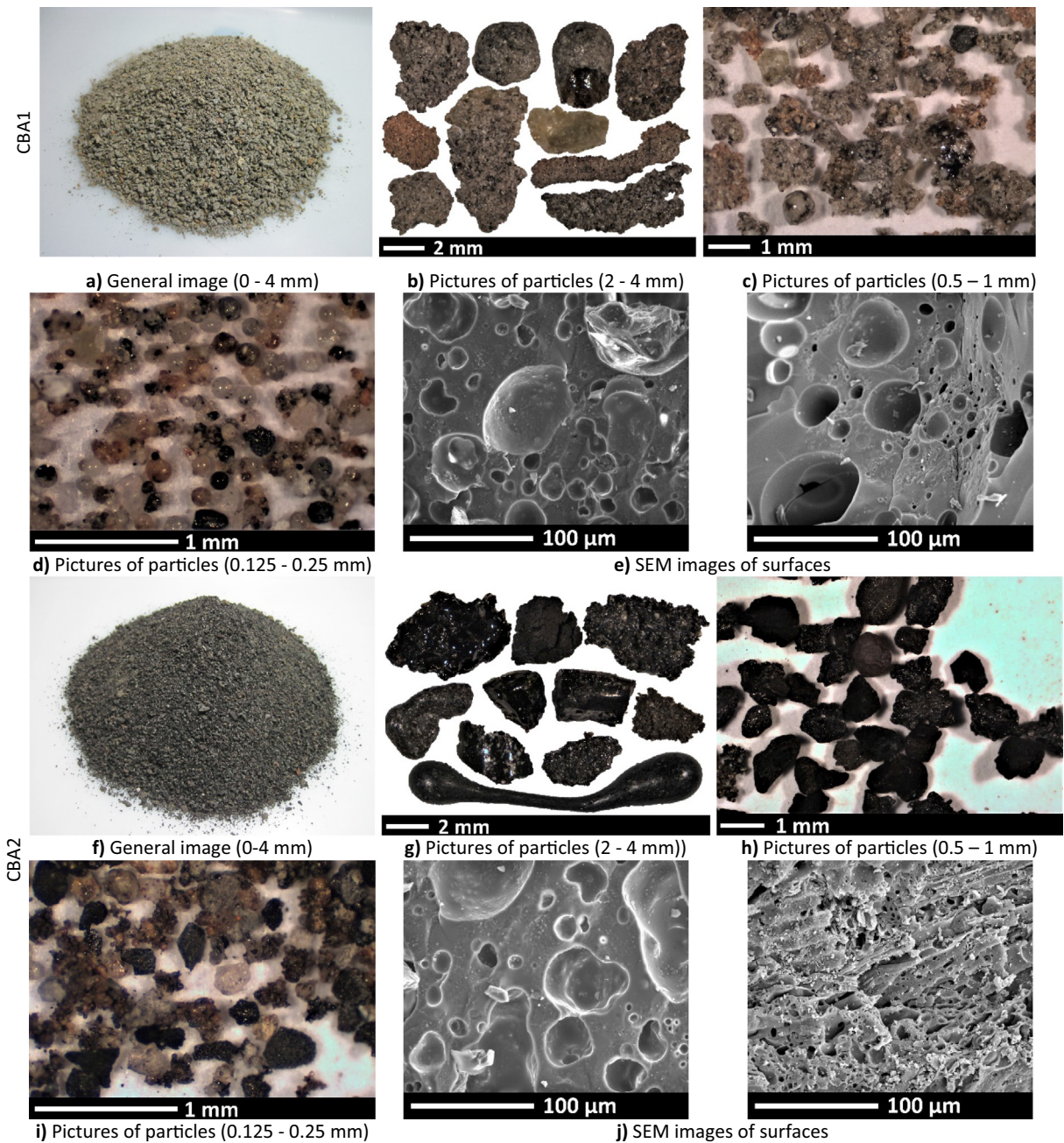


Fig. 4. Appearance, shape and texture of CBA1 and CBA2 particles.

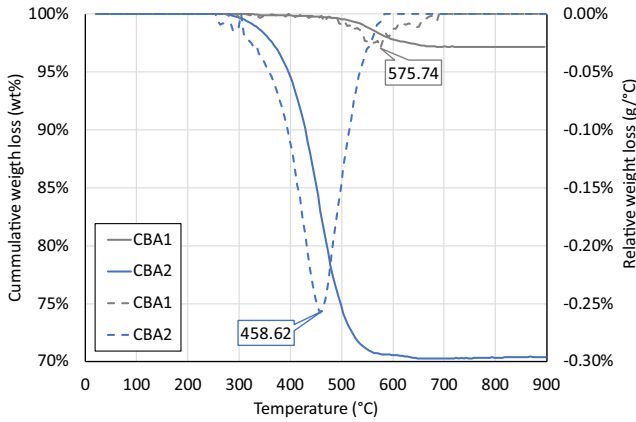


Fig. 5. TGA curves for CBA1 and CBA2.

The chemical compositions of CBA1 and CBA2 are shown in Table 1. Oxygen, silicon and aluminium are the most abundant chemical elements in both CBA1 and CBA2 followed by iron, calcium and others.

Some of the chemical elements are combined forming crystalline compounds, among which quartz and mullite are the most common (Fig. 6).

Size particle distribution, obtained according to UNE-EN 933-1 [65] of all the aggregates used and their corresponding fractions under 125 μm are shown in Fig. 7a and Fig. 7b.

The conventional aggregates were mixed in order to work with particle size distributions similar to those of the CBAs by which

Table 1  
Chemical composition by XRF (% in mass).

Oxides	CBA1	CBA2
SiO <sub>2</sub>	55.9	35.9
Al <sub>2</sub> O <sub>3</sub>	21.7	11.3
Fe <sub>2</sub> O <sub>3</sub>	6.4	12.3
CaO	5.4	7.4
Other	6.8	6.2
LOI	3.9	27.1

they are replaced in the mortars. Thus, FA1 and FA2 were combined at 70% and 30% respectively, to be replaced by CBA1 < 4 (Fig. 8) and FA1 and FA3 were combined at 45% and 55% respectively, to be replaced by CBA2 < 4 (Fig. 9).

In precast concrete, the conventional aggregates were mixed according to the indications of a precast concrete company: FA4, FA5 and CA were combined at 20%, 10% and 70% respectively. Then, a mix of conventional aggregates and CBA2 < 8 with a similar particle size distribution was designed: FA5, CA and CBA2 < 8 were mixed at 40%, 20% and 40% respectively (Fig. 10).

Other properties of conventional aggregates and sieved CBA1 and CBA2 are shown in Table 2.

CBA1 and CBA2 satisfy the requirements established for aggregates in the Spanish code for structural concrete (EHE [66]). According to this standard, the result of the sand equivalent test must be higher than 70 and the coefficient of friability must be lower than 40. Both wastes are also classified as non-reactive to silica and silicates as the registered expansions do not exceed 0.10%.

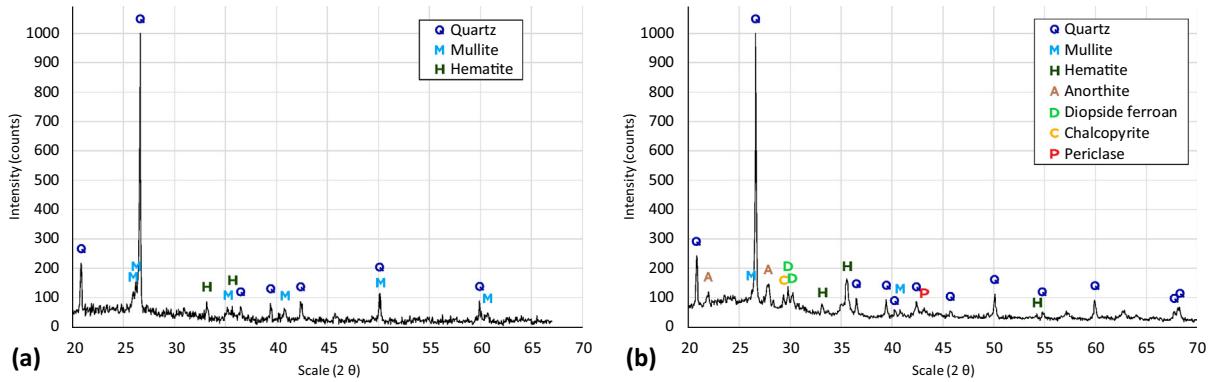


Fig. 6. X-Ray diffractograms of CBA1 (a) and CBA2 (b).

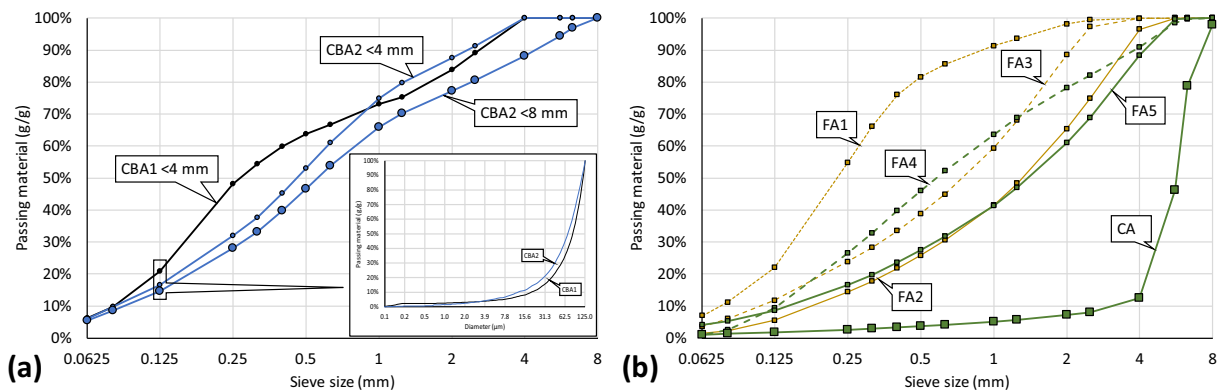


Fig. 7. Particle size distribution of (a) the CBA and (b) the conventional aggregates.

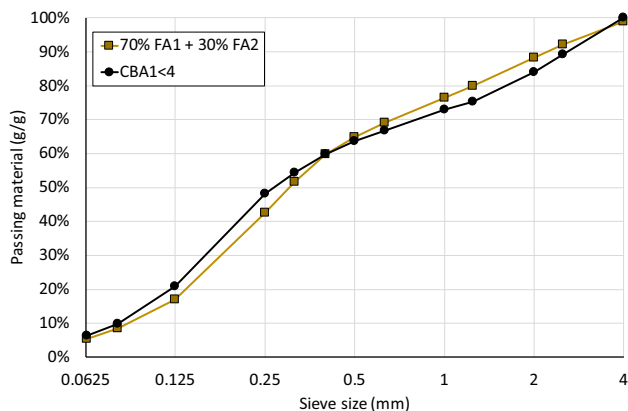


Fig. 8. Particle size distribution of CBA1 and the mixed conventional aggregate it replaces in mortars.

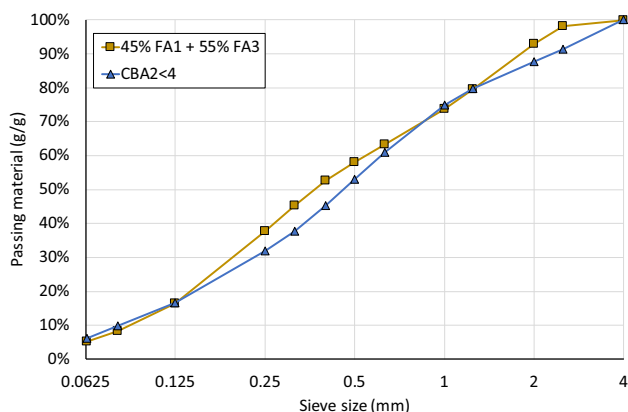


Fig. 9. Particle size distribution of CBA2 and the mixed conventional aggregate it replaces in mortars.

Masonry cement (MC) and fly ash blended cement (CEM II) are used as binders in this work. MC is named as MC 12.5 [73] and it is comprised of Portland cement clinker (41.3%) and other inorganic compounds (limestone 33.5%, calcined natural pozzolana 19.8% and gypsum 5.4%). CEM II is classified as CEM II A-V 42.5R [73] which means that its fly ash content is between 6% and 20% and it can contain up to a 5% of minor components. Detailed chemical composition of both binders is shown in Table 3.

The principal crystalline chemical compounds in the masonry cement are alite, belite, calcite and gypsum (Fig. 11a). In the fly ash blended cement, quartz and mullite are also detected (Fig. 11b).

Table 2  
Properties of the aggregates.

	Standard	Conventional aggregates						Coal bottom ashes			
		FA1	FA2	FA3	FA4	FA5	CA	CBA1<4	CBA2<4	CBA2<8	
Maximum size (mm)	EHE [66]	4	4	4	4	4	8	4	4	8	
Fineness modulus (-)	UNE 146,301 [67]	1.52	3.51	2.78	2.85	3.56	5.69	2.1	2.36	2.79	
Sand equivalent test	UNE-EN 933-8 [68]							94	71		
Specific gravity (g/cm <sup>3</sup> )	NY 703-19 E [69]	2.33	2.45	2.41	2.45	2.53	2.47	1.37	1.11	1.26	
Water absorption(wt%)	10 min 24 h	NY 703-19 E [69]	6.14	3.71	4.34	3.55	3.10	1.27	14.20	28.85	25.13
			6.15	3.71	4.42	3.65	3.13	1.43	17.39	40.35	33.29
Coefficient of friability of the sands	UNE 146,404 [70]							6	20		
Content of organic matter (wt%)	UNE 103,204 [71]							0.42	1.59		
Expansion due to alkali-silica and alkali-silicate potential reactivity (m/m,%)	UNE 146,508 [72]							0.03	0.07		

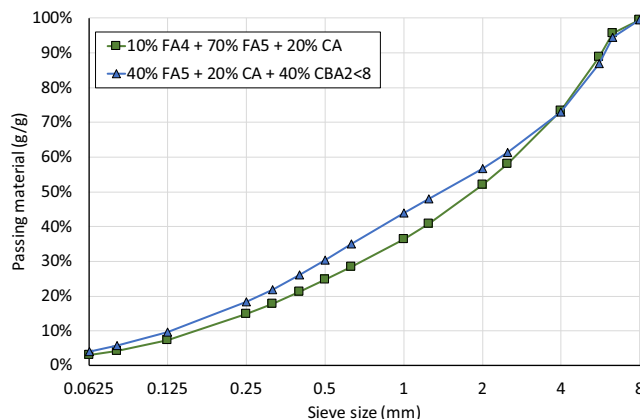


Fig. 10. Aggregates particle size distributions for the baseline mix and the higher substitution rate for PC.

MC and CEM II particle size distributions are shown in Fig. 12. Their specific surfaces are 3.61 m<sup>2</sup>/g and 1.30 m<sup>2</sup>/g, and their densities are 3.01 g/cm<sup>3</sup> and 3.02 g/cm<sup>3</sup>.

### 3. Methodology

#### 3.1. Mix proportions and masonry unit design

The separate use of CBA1 and CBA2 in masonry mortars (MM) and the use of CBA2 in precast concrete (PC) and masonry units (MU) are studied. Thus, three different series of materials (MM-CBA1, MM-CBA2 and PC) and a series of masonry units (MU) are manufactured. In MM, replacement rates of conventional sand with any of the two coal bottom ashes (CBA1 < 4 and CBA2 < 4) are established as 25%, 50% and 75% by volume. In precast concrete, using the aggregates shown in section 2, concretes were designed with an effective content of CBA2 < 8 in the total aggregate of 10%, 20%, 30% and 40%, also by volume.

The mix proportions of the baseline masonry mortars are established based on Martínez-García et al. [74]. The conventional precast concrete mix design is established based on company expertise. For any material and replacement rate, the paste to aggregate volume proportion and the mixing water to cement ratio are kept constant. The reduction of the mixing water due to absorption by conventional aggregates and CBA is minimized by wetting them during mixing (section 3.2). The amount of water used for this purpose (WAC-W) is equivalent to the aggregates water absorption capacity after 10 min when immersed in water (Table 2). The mix proportions of the three materials series (MM-CBA1, MM-CBA2 and PC) are shown in Table 4, Table 5 and Table 6.

MU consist of hollow blocks with two voids that fully penetrate the block (Fig. 13). The nominal dimensions of the MU are 400 mm

**Table 3**  
Cements chemical composition obtained by XRF (g/g).

	MC	CEM II
CaO	48.5%	53.4%
SiO <sub>2</sub>	17.9%	24.3%
Al <sub>2</sub> O <sub>3</sub>	6.1%	7.4%
Fe <sub>2</sub> O <sub>3</sub>	3.7%	2.0%
SO <sub>3</sub>	3.5%	2.6%
MgO	1.5%	5.0%
K <sub>2</sub> O	1.1%	0.9%
Na <sub>2</sub> O	0.6%	-
Other	0.6%	0.9%
LOI (975 °C)	16.5%	2.7%

in length, 200 mm in width and 200 mm in height, corresponding with the A series according to UNE 127771-3 [75]. Their manufacture dimensions are 397 + 1/-3 mm in length, 195 + 1/-3 mm in width and 192 ± 2 mm in height. Their solid ratio is 0.45 ± 0.5 and a minimum 25 mm width for the block walls is guaranteed [76]. Tolerances of all the reported dimensions correspond with the D2 class according to UNE-EN 771-3 [77]. MU with all the proposed PCs are manufactured in factory and tested in laboratory (Fig. 14).

3.2. Mixing procedure and curing conditions

The same mixing procedure was followed for casting masonry mortars and precast concrete, although different mixers were used. An 18 l capacity mixer is used for masonry mortars, whereas a 100 l capacity pan mixer is used for precast concrete. Aggregates, both conventional and coal bottom ash, were homogenized for 30 s while WAC-W was added. The mixer was then stopped and cement was added. 30 s later, mixing water was added and the process continued for 3 min. Therefore, the mixing process lasted 4 min. Two masonry mortar batches of 6 l and two precast concrete batches of 26 l were cast for each mix. Masonry units were manufactured in the company following the pre-established conventional procedure.

MM specimens were fabricated and immediately covered with a plastic bag for up to two days to minimize evaporation. Then they were demoulded and introduced again in the plastic bag for up to

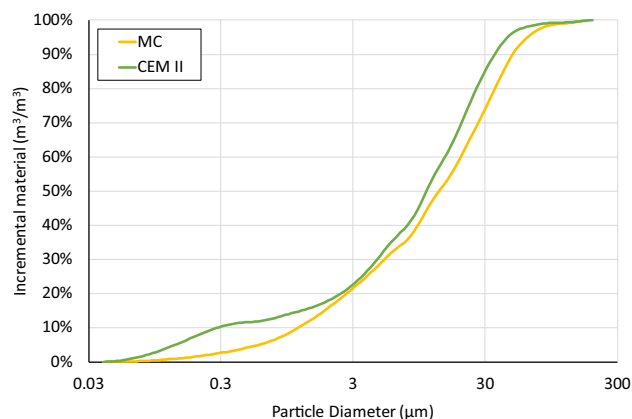


Fig. 12. Particle size distribution of binders.

five days. After that first stage (seven days), the specimens were taken out of their plastic bags and placed in a chamber at 24 ± 2 °C and 60 ± 5% RH. Precast concrete specimens were also covered with a plastic bag to minimize evaporation for up to they were demoulded (just three days after casting). After this first stage, the specimens were taken out of the plastic bag and placed in a chamber at 24 ± 2 °C and 60 ± 5% RH. The masonry units were cured in insulated chambers for 14 days and then exposed to environmental conditions (Fig. 15).

3.3. Testing methods

The workability of masonry mortars was studied by assessing the consistency using the flow table method and the plunger penetration method, while also assessing their workable life. The consistency is determined using the flow table according to UNE-EN 1015-3 [78] as the mean diameter of a mini-cone mortar slump that has been submitted to 10 table shakes. This test was carried out 10 min after mixing.

The consistency using the plunger penetration method is determined as the penetration into the mortar of a standard plunger falling freely from a standard height, according to UNE 1015-4

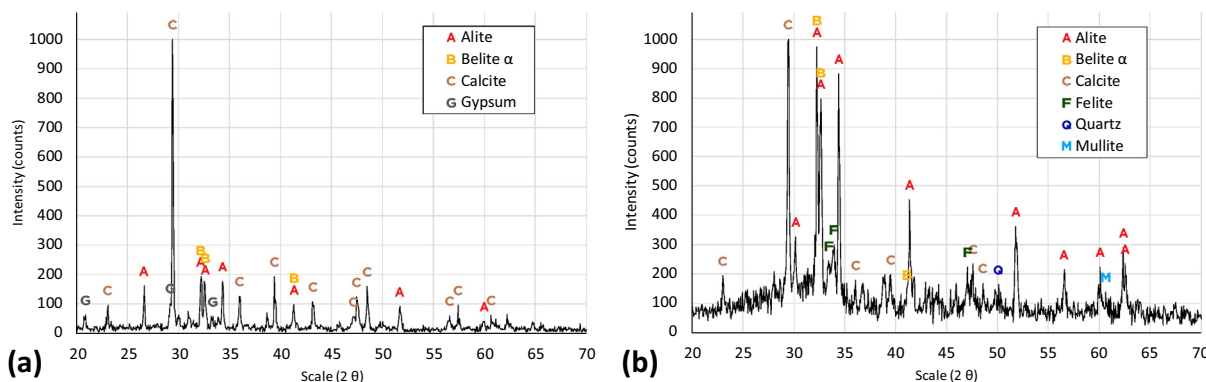


Fig. 11. X-Ray diffractograms of MC (a) and CEM II (b).

**Table 4**  
Mix proportions of MM-CBA1 (kg/m<sup>3</sup>).

	MC	Mixing water	FA1 + FA2	CBA1 < 4	WAC-W
MM-CBA1-0	445.93	251.85	1419.60	0.00	76.45
MM-CBA1-25	445.93	251.85	1064.70	210.00	87.16
MM-CBA1-50	445.93	251.85	709.80	420.00	97.86
MM-CBA1-75	445.93	251.85	354.90	630.00	108.57

**Table 5**  
Mix proportions of MM-CBA2 (kg/m<sup>3</sup>).

	MC	Mixing water	FA1 + FA3	CBA2 < 4	WAC-W
MM-CBA2-0	445.93	251.85	1424.80	0.00	72.95
MM-CBA2-25	445.93	251.85	1068.60	166.50	102.75
MM-CBA2-50	445.93	251.85	712.40	333.00	132.55
MM-CBA2-75	445.93	251.85	356.20	499.50	162.34

**Table 6**  
Mix proportions of PC (kg/m<sup>3</sup>).

	CEM II	Mixing water	CA + FA4 + FA5	CBA2 < 8	WAC-W
PC-0	212.92	69.74	2165.29	0.00	60.17
PC-10	212.92	69.74	1949.01	108.70	80.54
PC-20	212.92	69.74	1732.39	217.39	100.90
PC-30	212.92	69.74	1515.79	326.09	121.25
PC-40	212.92	69.74	1299.18	434.78	141.61

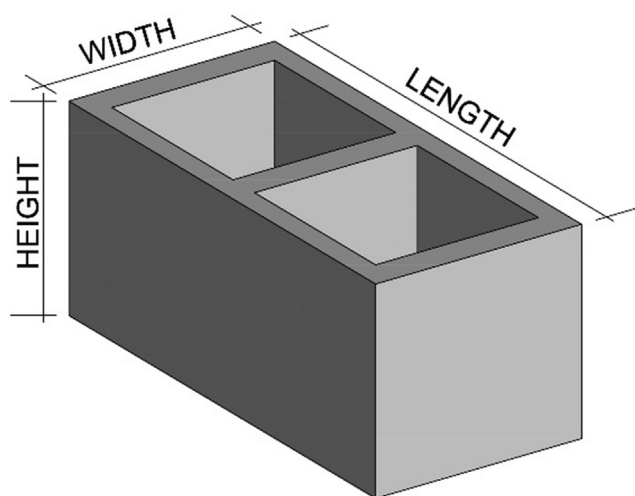


**Fig. 13.** Simplified geometry of a MU.



**Fig. 14.** Stored MU.



**Fig. 15.** Curing place for masonry units.

the factory when producing masonry units. Two cylindrical moulds of dimensions Ø15x30 mm are half filled with concrete and vibrated for 20 s. One of them also contains a 20 kg weight that compresses the concrete while the vibration occurs. The difference between the initial and final height of the concrete in the moulds is used as an indicator for the workability of concrete. The test was carried out for the two precast concrete batches of each mix.

Bleeding is another important fresh state property to be assessed in masonry mortars. The procedure followed in this case is based on UNE-EN 480-4 [80]. This standard describes a test for concrete, so the dimensions of samples and equipment used were adapted. A 1 l sample is kept in a cylindrical container after its filling with three layers tapped 10 times each with a rod. Bleeding water is periodically collected with a pipette from the mortar's surface. The sample remains covered with a lid between measurements. The test was carried out with one sample from each mortar batch.

The workable life period is determined according to UNE-EN 1015-9 [81] as the time that the mortar takes to acquire a specific resistance to penetration by a standard rod. A container is filled with mortar in 10 steps and beaten against a table four times after each step. Once full, the container remains in a plastic bag to avoid water evaporation and is only taken out in order to carry out a penetration resistance measurement. The penetration resistance measurements are repeated after different time periods until a standard value is exceeded. Then, time for the standard penetration resistance value is interpolated and considered as the mortar's workable life period. This test was carried out on two samples of each mix but only for masonry mortars with CBA2.

The rise of temperature in masonry mortars due to cement hydration was recorded using a thermometer in a non-

[79]. This test is executed two and a half minutes after the mixing ends.

The workability of precast concrete is assessed by a test that tries to simulate the compaction procedure that takes place in

**Table 7**

Testing programme. (X · Y = Z; X = Number of batches made of each mix; Y = Number of specimens made from each batch; Z = Number of specimens made of each mix).

		MM-CBA1	MM-CBA2	PC-CBA2	MU-CBA2
Workability and heat of hydration	Flow table	2 · 1 = 2	2 · 1 = 2	-	-
	Plunger penetration	2 · 1 = 2	2 · 1 = 2	-	-
	Compaction ease by vibration	-	-	2 · 1 = 2	-
	Compaction ease by vibration with weight	-	-	2 · 1 = 2	-
	Bleeding	1 · 2 = 2	1 · 2 = 2	-	-
	Workable life	-	1 · 2 = 2	-	-
	Heat of hydration	-	1 · 1 = 1	-	-
Density, air content and structure	Densities of fresh material	2 · 10 = 20	2 · 10 = 20	2 · 10 = 20	-
	Density of hardened material at the age of 28 days	1 · 2 = 2	1 · 2 = 2	1 · 2 = 2	-
	Air content	2 · 1 = 2	2 · 1 = 2	-	-
	Porosity at the age of 28 days	1 · 2 = 2	1 · 2 = 2	1 · 2 = 2	-
	Microscopy at the age of 90 days	Several	Several	-	-
Mechanical performance	Compressive strength at the age of 3, 7, 14 & 28 days (& 90 days for PC)	1 · 4 = 4	1 · 4 = 4	1 · 2 = 2	1 · 5 = 5
	Flexural strength at the age of 3, 7, 14 & 28 days	1 · 2 = 2	1 · 2 = 2	-	-
	Splitting-tensile strength at the age of 28 days	-	-	1 · 2 = 2	-
Volume stability	Length change in hardened state	1 · 3 = 3	1 · 3 = 3	-	-
Durability	Water absorption by immersion	1 · 2 = 2	1 · 2 = 2	1 · 2 = 2	1 · 5 = 5
	Water absorption due to capillary action	1 · 6 = 6	1 · 6 = 6	1 · 2 = 2	1 · 5 = 5

standardized semi-adiabatic calorimeter from 15 min after cement–water contact. This test was carried out once for each masonry mortar mix with CBA2.

The fresh density of mortar and precast concrete was assessed based on UNE-EN 1015-6 [82]. All specimens cast for strength and durability tests were weighed and their weights divided by the volumes of the moulds. At 28 days old, two pieces of each mix were extracted from a whole specimen and submitted to con-

ditions according to UNE 83,980 [83]: oven drying at 110 °C to constant mass, wetting by immersion to constant mass and immersion in boiling water for 5 h. After each of these steps, the surface dry weight of the specimens was recorded. Finally, their apparent mass in water was measured. Combining all the registered data, the apparent dry density, density after immersion and boiling, pore volume accessible for water after immersion (PVI) and pore volume accessible for water after boiling (PVB) were obtained.

The air content of mortars in fresh state is assessed by the procedure described in UNE-EN 1015-7 [84]. A standard container is filled with mortar in four 10-times-tapped layers. The container is sealed with a lid equipped with an air chamber and manometer. Water is introduced into the container until full. Pressure is applied to the air chamber and then this pressure is released until it equilibrates with the container. The difference between the initial and final pressure in the air chamber is related to the air content in the mortar. This test was carried out for one sample of each mortar batch.

In order to examine other aspects of the structure of the mortars, pictures of cut surfaces at different visual magnifications were taken with a LEICA DM750M microscope at 90 days.

The mechanical properties of masonry mortars were tested according to UNE-EN 1015-11 [85] at 3, 7, 14 and 28 days. Two specimens of each mix, with dimensions 160x40x40 mm, were first submitted to a constantly increased load (20 kN/s) in a three-point flexural strength test setup. When split into halves, they were submitted to a constantly increased load (150 kN/s) in

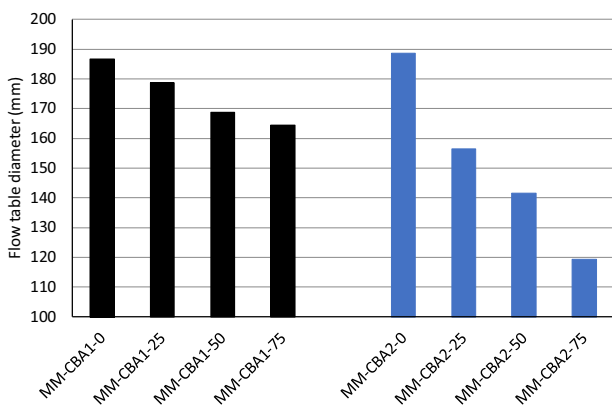


**Fig. 16.** Mortar flow table diameter (mm).

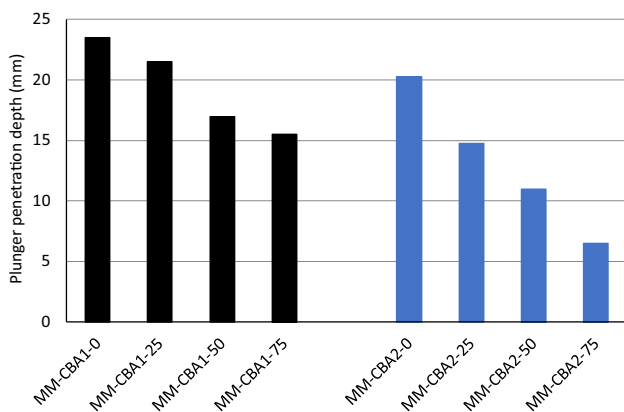


**Fig. 17.** Plunger penetration depth in mortar (mm).

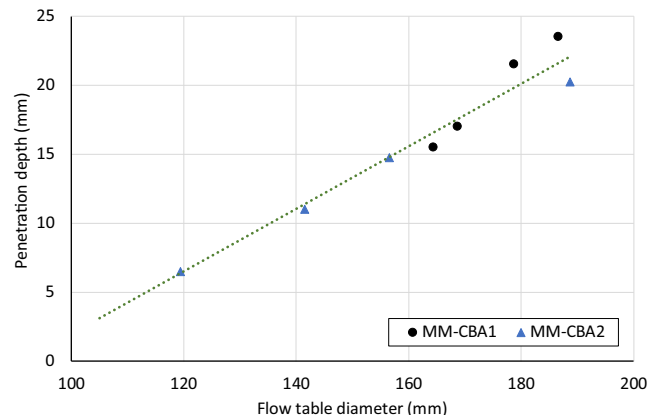


**Fig. 18.** Linear correlation between flow table diameter and plunger penetration depth in mortar mixes.



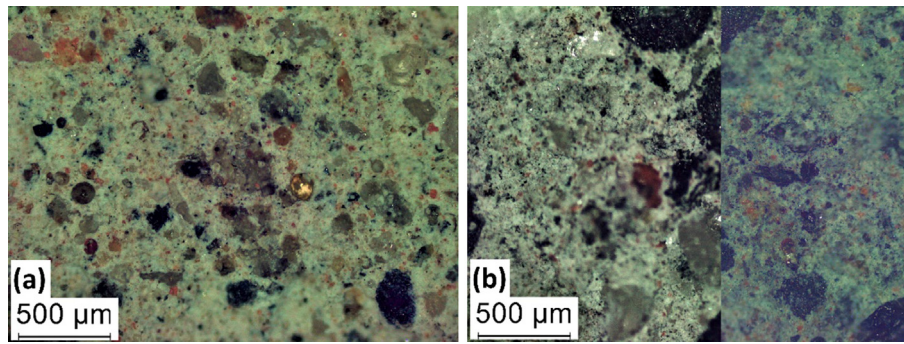


Fig. 19. Pictures of (a) MC-CBA1-75 and (b) MC-CBA2-75.

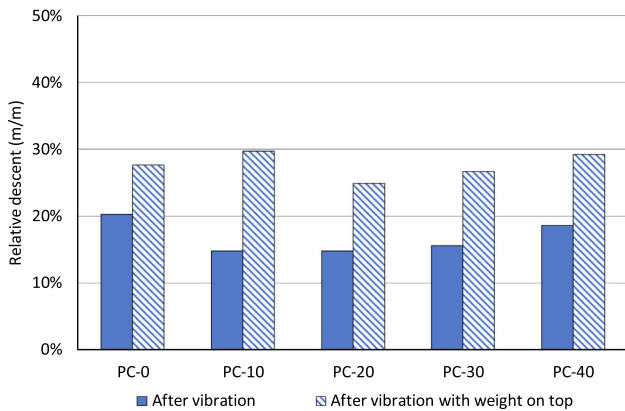


Fig. 20. Relative descent of precast concrete when submitted to vibration or vibration with a weight on top.

a compressive strength test setup. Regarding precast concrete, the compressive strength was obtained according to UNE-EN 12390-3 [86] at 3, 7, 14, 28 and 90 days. Two cubic specimens of each mix, 100 mm in width, were submitted to a progressive load at an increase rate of 4 kN/s. The 28-day splitting-tensile strength was assessed according to UNE-EN 12390-6 [87]. Two cylindrical specimens of each mix, with dimensions  $\varnothing 15 \times 30$  mm, were longitudinally loaded at an increase rate of 0.7 kN/s. The compressive strength of masonry units was tested on five units per mix at 3, 7, 14 and 28 days following the UNE-EN 772-1 [88]. The normalized compressive strength was obtained by applying a shape factor (0.14) according to the same standard.

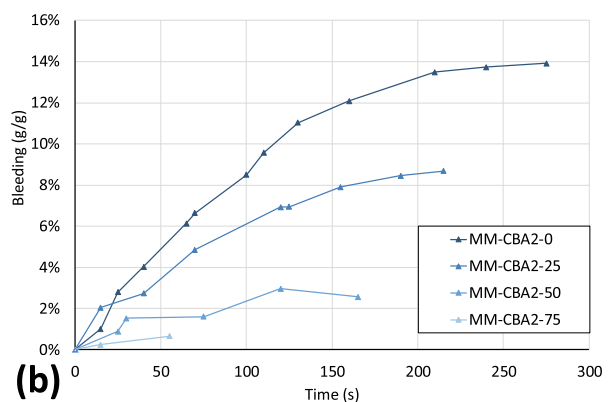
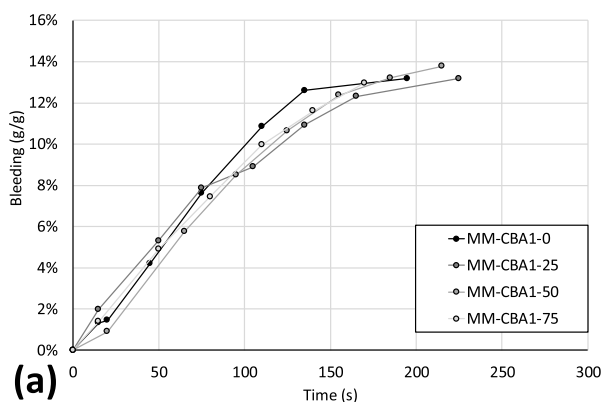


Fig. 21. Bleeding over time of (a) MM-CBA1 and (b) MM-CBA2 series.

The durability of the masonry mortars, precast concrete and masonry units was evaluated through the water absorption by immersion and water absorption due to capillary action methods. For the water absorption by immersion method, two specimens and five masonry units of each mix were tested. Furthermore, water absorption due to capillary action was obtained according to UNE-EN 1015-18 [89], UNE 83,982 [90] and UNE-EN 772-11 [91] for hardened mortar, precast concrete and masonry units, respectively. Six mortar specimens, two precast concrete specimens and five masonry units of each mix were used. The mortar specimens are halves of  $40 \times 40 \times 160$  mm specimens obtained by splitting in a flexural test setup. Precast concrete specimens are pieces obtained after splitting-tensile tests. They are all then immersed in water up to 5 mm in depth with the fracture surface facing down. Lateral surfaces are protected from wetting with paraffin. The coefficient is the water absorption rate from 10 to 90 min of immersion.

The length change up to 90 days of three specimens of each mortar mix, with dimensions  $40 \times 40 \times 160$  mm, were recorded with a digital dial attached to a linear transducer based on UNE-EN 12617-4 [92]. Measurements were taken when the specimens were kept in plastic bags (first seven days after demoulding) and, after that, while exposed to a 60% RH environment. The weight loss of the specimens was recorded after each length measurement.

The testing programme is summarized in Table 7.

#### 4. Results and discussion

The results obtained for masonry mortars, precast concrete and masonry units with CBA are grouped into five categories: workability, density and porosity, strength, length change and durability. The three materials are jointly analysed in each group. This

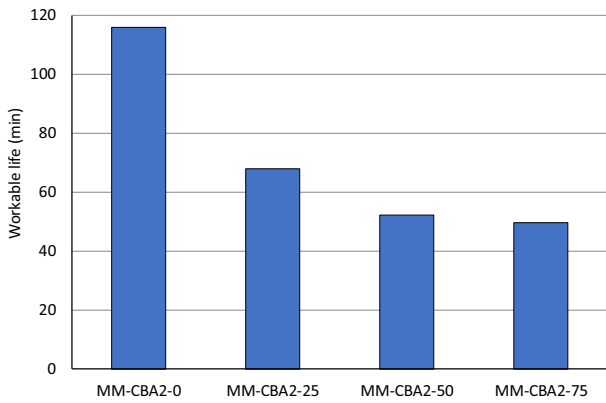


Fig. 22. Workable life of masonry mortars with CBA2.

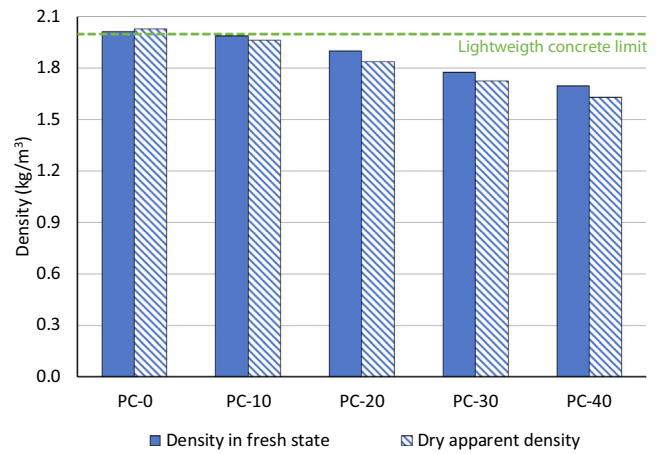


Fig. 25. Density in fresh state and dry apparent density of precast concrete.

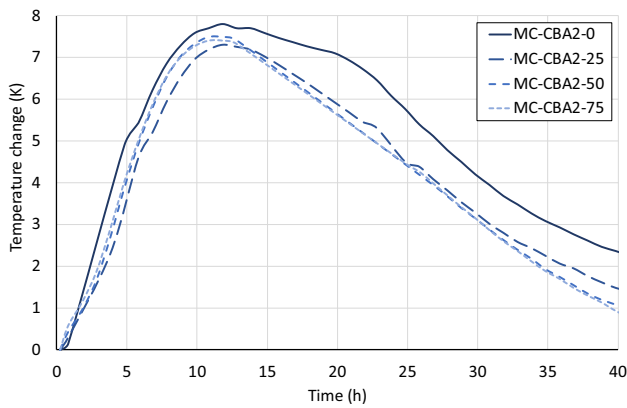


Fig. 23. Temperature of masonry mortars registered in a semi-adiabatic calorimeter.

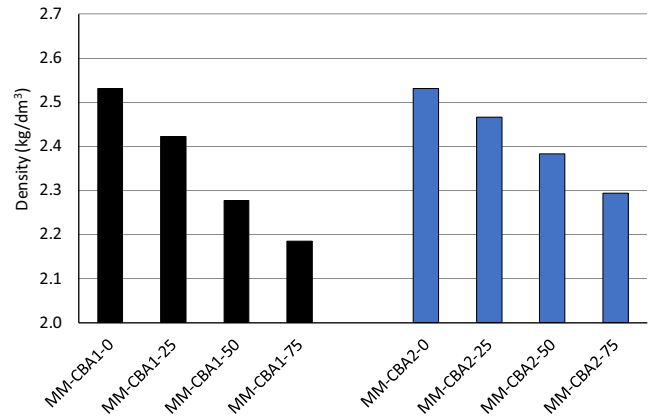


Fig. 26. Density after immersion and boiling of masonry mortars.

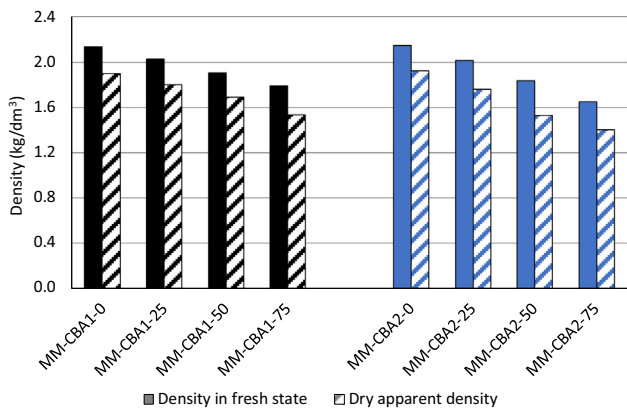


Fig. 24. Density in fresh state and dry apparent density of masonry mortars.

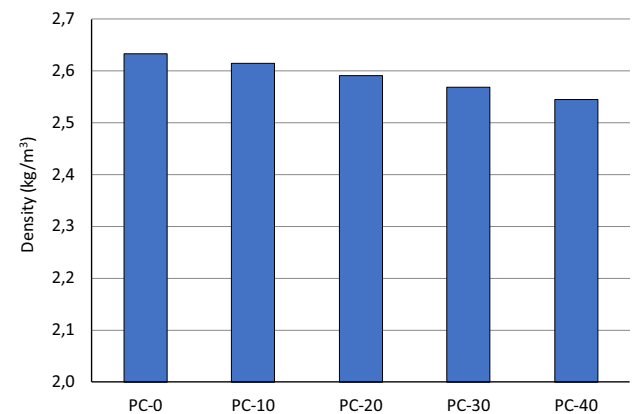


Fig. 27. Density after immersion and boiling density of precast concrete.

discussion scheme is chosen so the effects of CBA on masonry mortars, precast concrete and masonry units can be compared.

#### 4.1. Workability and heat of hydration

The workability of masonry mortars decreases when either the content of CBA1 or CBA2 is increased. This can be stated in view of the results obtained in the flow table test and the plunger test, which reported a reduction in the spread diameter and penetration depth respectively (Fig. 16 & Fig. 17).

A good correlation is found between both tests (Fig. 18). However, they do not converge at their minimum possible records (100 mm for flow table and 0 mm for plunger penetration) because of the gap between their execution times (see section 3.2).

The higher inter-particle friction due to the irregular shape and rough surface of the CBA decreases the workability of mortars. The presence of fine rounded particles in MM-CBA1 contributes to lighter reductions in fluidity than in MM-CBA2 (Fig. 19 a & b).

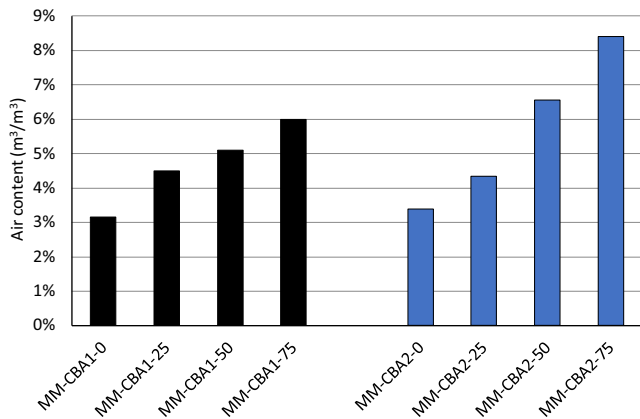


Fig. 28. Air content of masonry mortars.

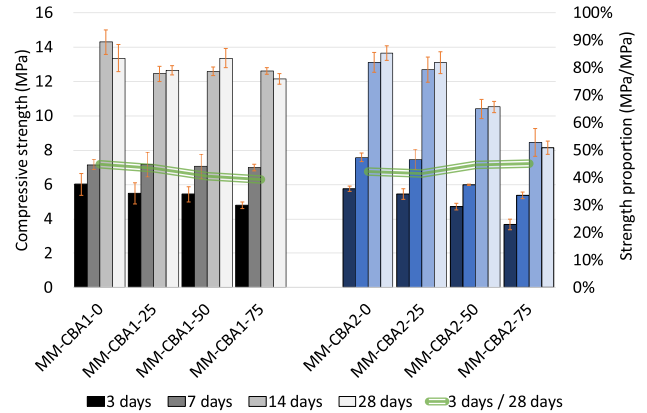


Fig. 31. f<sub>c</sub> of masonry mortars.

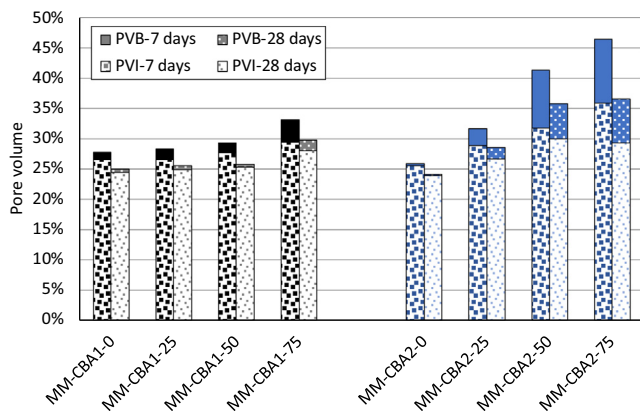


Fig. 29. PVI and PVB in masonry mortars.

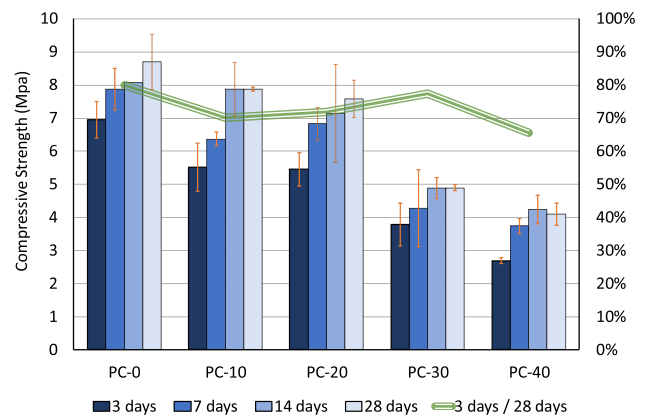


Fig. 32. f<sub>c</sub> of precast concrete.

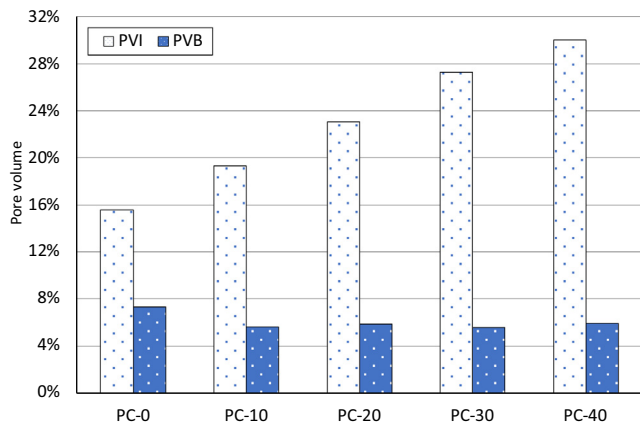


Fig. 30. PVI and PVB in precast concrete.

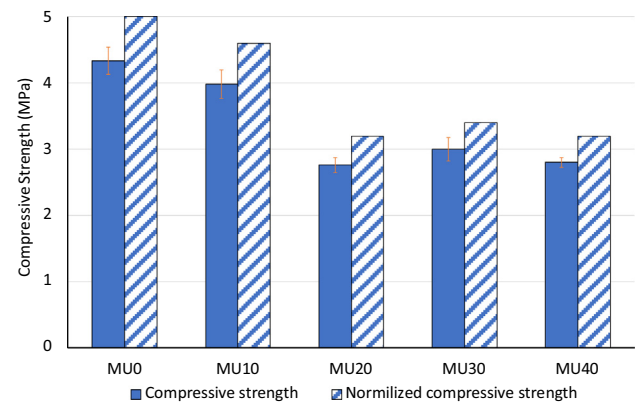


Fig. 33. f<sub>c</sub> of masonry units at 28 days.

Furthermore, the reduction of the mixing water due to the ongoing absorption by the CBA highly absorbent particles also decreases the workability. The absorption effect was mitigated to some extent by the addition of WAC-W. However, this measure might not be enough to prevent ongoing water absorption, especially by CBA2 particles. This is believed to be the main reason for the higher reduction in workability in the mortars with this ash. Each 25% increase in the content of CBA1 shows an average decrease of 7.4 mm for the flow table diameter and 2.7 mm for

the plunger penetration depth. When CBA2 is used, the corresponding drops are higher: 20.9 and 4.2 mm respectively.

Precast concrete is characterized by a very low mixing water content, so a small amount must be available for possible absorption by the aggregates. Therefore ongoing water absorption by CBA2 seems to be negligible in precast concrete, as no clear trend can be established from the workability results (Fig. 20).

The results of bleeding in the mortar specimens supports the aforementioned idea of ongoing water absorption of CBA2. The mortars with CBA1 exhibit a similar amount of accumulated bleeding water and a similar final bleeding time (Fig. 21 a). However, the

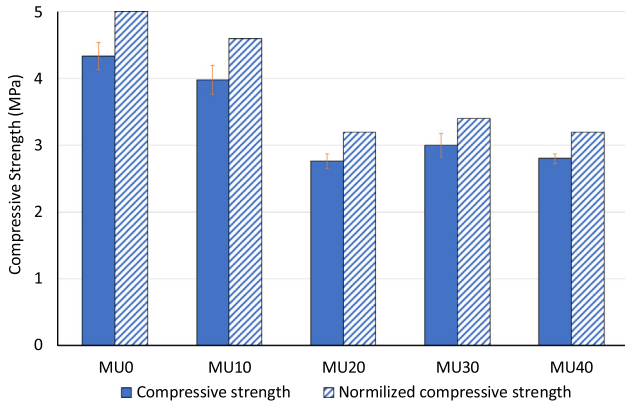


Fig. 34. Flexural strength of masonry mortars.

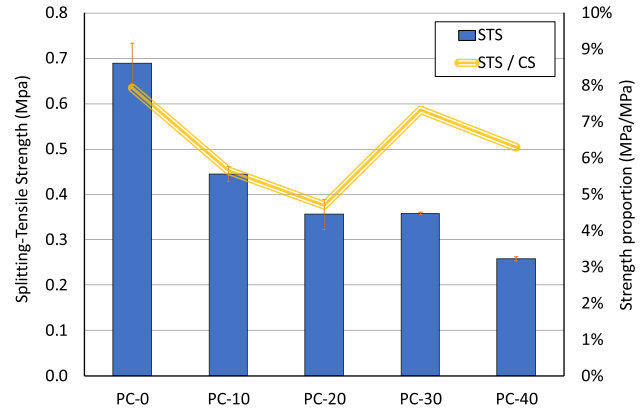


Fig. 35. Splitting-tensile strength of precast concrete at 28 days.

bleeding water and times decrease when the CBA2 content increases due to the ongoing water absorption and consequent reduction in the water to cement ratio (Fig. 21 b).

The authors believe that the decrease in the workable life period of the mortars with CBA2 (Fig. 22) supports the existence of a noteworthy ongoing water absorption after mixing, despite the fact that every mortar starts its workable life from a different workability. However, the effect is less significant when high replacement rates are used where similar workable life periods are recorded. The increase in the water demand by the CBA can only be satisfied with mixing water up to a certain point. It is harder for the mixing water to get into the CBA when it is severely reduced. Thus, the effect of the ongoing water absorption tends to be minimized. This argument is analogous to the one used when discussing the maintenance of workability in precast concrete.

Any relationship between changes in the workable life period and the possible effects of CBA on the cement early hydration has been dismissed. The use of CBA is believed not to significantly influence cement hydration as the temperature evolution in the semi-adiabatic calorimeter follows the same trend for any replacement rate (Fig. 23).

The “incomplete saturation” of CBA2 must be related to the fact that the test for determining water absorption depends on the accurate determination of a saturated surface dry condition, which is quite challenging.

4.2. Density, air content and structure

The use of CBA decreases the density of masonry mortars and precast concrete in both fresh and hardened state (Fig. 24 and Fig. 25). The difference between the fresh density and the dry apparent density is attributed to the water loss that takes place when the curing conditions of both materials change (from inside

a plastic bag to a 60% RH environment, as explained in section 3.3). Precast concrete with any CBA2 content can be considered light-weight concrete in terms of density according to EHE [66].

The light weight of CBA particles in comparison to conventional aggregates, even when wet, explains the decrease in density when they are used. This specific characteristic is reported when studying the CBA particles themselves and also when studying the density after immersion and the boiling of mortars (Fig. 26) and precast concrete (Fig. 27).

The use of CBA increases the air content (Fig. 28) in the masonry mortars, which also leads to a decrease in density. The air in the mortars is present in both the aggregates (if not completely saturated) and the paste. The air in the aggregates can move to the paste when they absorb mixing water and remain in it forming bubbles, if they do not reach the surface of the fresh material. Furthermore, entrapped air can also be introduced into the mortar because of the irregular shape of CBA.

The results regarding the pore volume corroborate the trend for the air content. The PVI increases when the CBA content increases. However, this occurs more remarkably in mixes with CBA2 (Fig. 29 & Fig. 30). PVB trend is similar to PVI in materials with any content of any of the two ashes, excluding mortars with a 50% or higher replacement rate of CBA2, where it is higher. This disruptive performance could be due to a higher porosity in the interfacial transition zone related to the desorption of water from the CBA particles. Both PVI and PVB decrease from 7 to 28 days, indicating that pores allocated in the paste are progressively filled with cement hydration products.

4.3. Strength

The compressive strength ( $f_c$ ) decreases when the CBA content increases due to the weakness of the CBA particles themselves

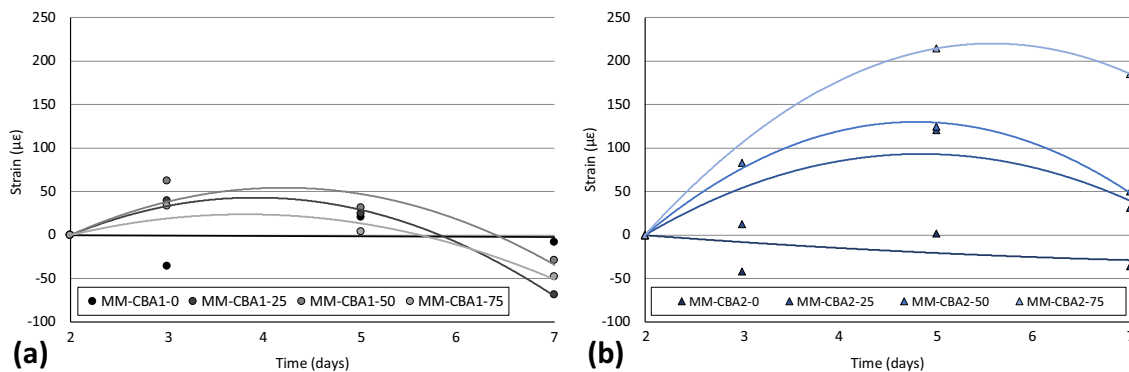


Fig. 36. Length change of masonry mortars containing CBA1 (a) and CBA2 (b).

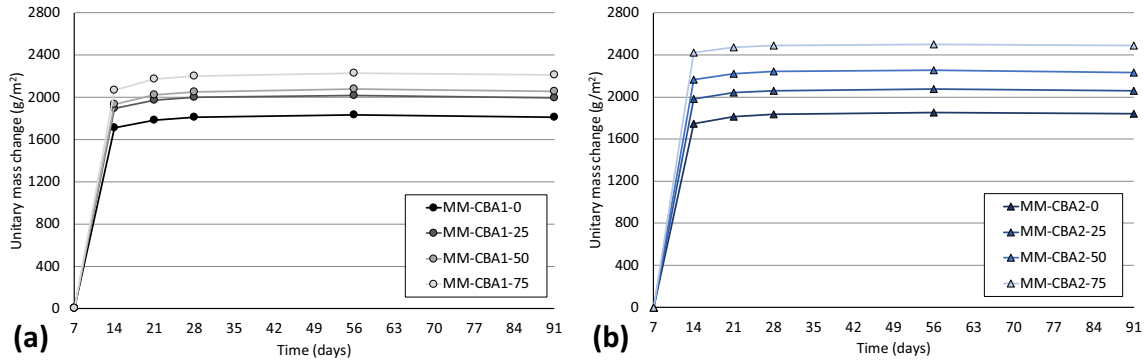


Fig. 37. Weight loss of mortars containing CBA1 (a) and CBA2 (b).

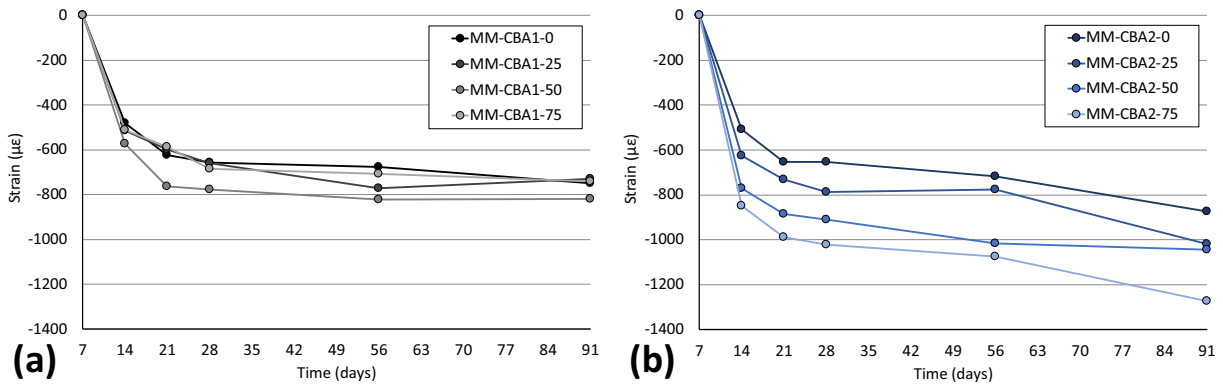


Fig. 38. Shrinkage in drying conditions of masonry mortars containing CBA1 (a) and CBA2 (b).

and the higher pore volume generated when they are used. However, when a low content of any of the two ashes is used, low  $f_c$  reductions are reported. For instance, the 28-day  $f_c$  decreases up to a 5.4% and 4.0% in mortars with a 25% replacement ratio of CBA1 and CBA2, respectively (Fig. 31). Precast concrete reduces its 28-day  $f_c$  up to 12.8% when a 20% replacement rate is used (Fig. 32) and masonry units with 8.0% less  $f_c$  than the reference were obtained with a 10% replacement rate (Fig. 33). The effect of the two ashes significantly differs for higher replacement rates. For instance, the mortars with CBA1 suffer a slight reduction (9.0%) for the 75% replacement rate in comparison to the conventional mortar. On the other hand, the drop is drastic (40.5%) for the same case when CBA2 is used. The notable difference must be related to the higher PVB when CBA2 is used at replacement rates higher

than 25%. This phenomenon might be related to a worse interfacial transition zone in CBA particles as explained in the previous section. The precast concrete with the highest content of CBA2 reaches a 28-day  $f_c$  reduction of 52.8%. The masonry units with the same proportion of the by-product reduce their  $f_c$  up to 36.0% with respect to the reference.

The flexural strength of the masonry mortars follows a trend parallel to the  $f_c$ . It decreases slightly when CBA1 or low replacement rates of CBA2 are used, whereas the decrease is more noteworthy if high contents of CBA2 are used (Fig. 34).

The evolution of compressive and flexural strength over time is similar for all mixes (Fig. 31, Fig. 32 & Fig. 34). Therefore, any influence of the CBA particles on cement hydration (possible internal

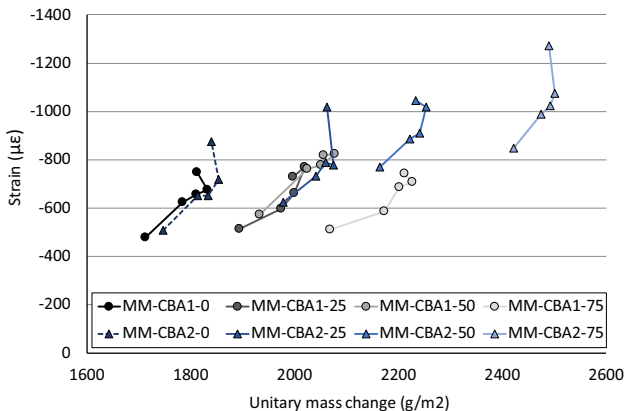


Fig. 39. Relationship between unitary mass change and shrinkage in drying conditions.

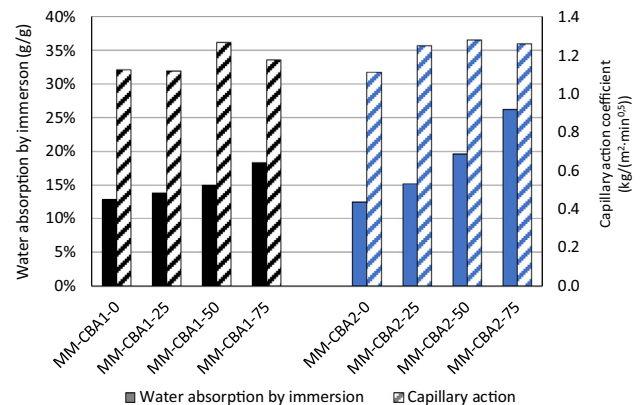


Fig. 40. Water absorption by immersion and water absorption by capillary action in masonry mortars.

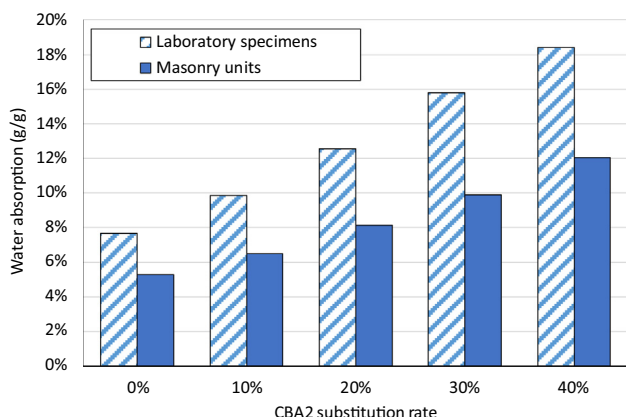


Fig. 41. Water absorption by immersion in precast concrete laboratory specimens and masonry units.

curing) or paste porosity evolution (possible pozzolanic reactions) does not play a significant role in strength development in this type of materials with a relatively high water to cement ratio. The porosity and weakness of the CBA particles themselves and the porosity increase due to air entrapment during compacting are the predominant causes for the decrease in strength.

The splitting-tensile strength of precast concrete also decreases when the CBA content increases (Fig. 35). The detrimental effect is high even for the lowest replacement rate, with a 35.5% drop being recorded in this case.

The relationship between  $f_c$  and flexural strength FS in masonry mortars and between  $f_c$  and splitting-tensile strength in precast concrete is similar for all the replacement rates (Fig. 34 & Fig. 35).

#### 4.4. Volume stability

The strain of the mortar specimens for the period during which they were kept in plastic bags is plotted in Fig. 36 a & b. This deformation is considered an autogenous strain as the specimens could only exchange a minimum amount of humidity with the surrounding environment while the measurements were taken. Conventional mortars and mortars with CBA1 show a quite stable performance. However, the mortars with CBA2 experimented some swelling. Autogenous swelling can be caused by different phenomena, of which the migration of WAC-W and absorbed mixing water from the CBA2 to the paste is believed to be the predominant in this case. The migration of such an amount of water that is able to cause swelling is possible due to the high water absorption capacity of CBA2 particles but also to their water desorption capacity. Therefore, the development of autogenous swelling depends on the aggregates water desorption capacity, which is believed to be high for CBA2 and low for CBA1 based on the obtained results. Then, CBA2 is considered to be able to work as an internal curing water reservoir. Internal curing is the supplying of water within a cementitious mixture using pre-wetted lightweight aggregate, or other materials that readily release water from within their particles, thereby mitigating self-desiccation and sustaining hydration [93]. Some factors such as a lower modulus of elasticity (assumed from strength results) must have also promoted a larger deformation.

When the masonry mortar specimens are taken out of the plastic bags and exposed to a 60% RH environment, they lose weight due to water evaporation (Fig. 37 a & b). The quick water release is promoted by the high surface to volume ratio of the specimens, which can be representative of the real life situation for masonry mortar in field application. The weight decrease is higher when the CBA content increases, especially when CBA2 is used, due to the higher initial total water content (mixing water + WAC-W).

The loss of water causes drying shrinkage. Thus, drying shrinkage is higher when higher replacement rates are used and especially when CBA2 is used (Fig. 38 a & b). A lower modulus of elasticity of mixes with CBA2 (assumed from strength results) is also believed to influence the results.

Graphs resulting from plotting strain against unitary mass change, trace a similar shape for any replacement rate (Fig. 39). The first stage is defined by a positive linear relationship between the unitary mass change and the strain. A second stage is defined by an increase of shrinkage while the weight remains constant or even increases. The latter performance is due to the coexistence of drying and carbonation processes. Drying implies mass loss and volume reduction, whereas carbonation implies mass gain ( $\text{CO}_2$  uptake) and volume reduction. The sum of the two phenomena produces shrinkage and can result in a reduction, increase or balance with regards to weight change.

#### 4.5. Durability

Water absorption of masonry mortars, precast concrete and masonry units increases if the CBA content increases (Fig. 40 & Fig. 41). This effect is more pronounced when CBA2 is used as it increases porosity more significantly (section 4.2). The capillary action in masonry mortars remains similar for all the replacement rates for CBA1 and CBA2 (Fig. 40). This performance is attributed to the simultaneous increase of both PVI and PVB. PVI is believed to be predominantly composed of pores with a large diameter, whereas PVB is believed to be predominantly composed of pores with a small diameter. The two kinds of pores promote water absorption by immersion. However, the water absorption due to capillary action is promoted by pores with a small diameter while hindered by pores with a large diameter. The effect of PVI and PVB might compensate each other regarding capillary uptake. Thus, a similar coefficient for all the different contents of CBA in mortars is obtained. Furthermore, it must be noted that the precast concrete specimens manufactured in the laboratory exhibit higher water absorption than factory made masonry units (Fig. 41). Both are made of the same precast concrete, however, better compaction in the factory leads to lower porosity.

#### 5. Conclusions and future line of research

Based on the discussed results, it can be concluded that a higher replacement rate of conventional aggregate with wetted CBA has the following effects on masonry mortars, precast concrete and masonry units:

- Workability decreases due to the irregular shape and the ongoing water absorption of the CBA. This absorption is minimized if the ash particles are effectively saturated or if mixing water is not available to be absorbed. The bleeding test can be used to evaluate CBA water absorption after mixing with successful results.
- Porosity increases due to the high porosity of CBA particles and the entrapment of air during mixing due to their irregular shape. Density decreases as porosity increases.
- Strength decreases due to the weakness of the CBA particles themselves and the pores they produce. However, acceptable values for masonry mortars and units are achieved for low contents.
- Weight loss and shrinkage of masonry mortars increase in air-drying curing conditions due to the increase in the total water content in the mixes (CBA is used in SSD condition). Some autogenous swelling is detected up to 7 days when CBA2 is used, while the mixes are kept in plastic bags.

- Water absorption by immersion increases due to the increase in porosity, although, water absorption due to capillary action remains constant in masonry mortars. The latter may be explained by the type of pores produced by the CBA. It generates both large and small pores which hinder and favour capillary suction respectively.

In general, CBA1 shows better performance than CBA2 as an aggregate in masonry mortars. Its use leads to less detrimental effects on workability, and mechanical and durability properties. However, acceptable results are obtained when a low content of any of the two proposed ashes is used. Further research on other properties of masonry mortars is recommended, such as water permeability and adhesive strength on substrates, in order to confirm the feasibility of the two types of CBA in this kind of material. The density decrease that has been detected in any of the studied materials is especially valued in masonry units. It eases handling and reduces the thermal conductivity of these elements and therefore improves their economic, environmental and functional performance. However, the use of CBA decreases the strength of masonry units, so high replacement rates might only be acceptable for non-structural applications. Furthermore, some autogenous swelling was detected in masonry mortars containing CBA2, suggesting that this ash could work properly as an internal curing water reservoir. Internal curing is especially convenient in high performance concrete with a low water to cement ratio. Therefore, the use of CBA2 as an internal curing water reservoir in high performance concrete is proposed as a promising advanced application of this by-product.

#### CRediT authorship contribution statement

**Roberto Rodríguez-Álvarez:** Conceptualization, Formal analysis, Investigation, Writing - original draft, Visualization. **Belén González-Fontebao:** Formal analysis, Investigation, Writing - review & editing, Supervision. **Sindy Seara-Paz:** Formal analysis, Investigation, Writing - review & editing, Supervision. **Emilio José Rey-Bouzón:** Formal analysis, Investigation.

#### Declaration of Competing Interest

The authors declare that they have no known competing financial interests or personal relationships that could have appeared to influence the work reported in this paper.

#### Acknowledgements

This work has been carried out within the framework of the following projects:

- HACCURACEM project (BIA2017-85657-R), funded by the Ministry of Economy, Industry and Competitiveness, State Program for Research, Development and Innovation aimed at the challenges of Society, within the framework of the State Plan for Scientific and Technical Research and Innovation 2013-2016, Call 2017.
- Valorisation of coal ashes from thermal power plant through the development of sustainable materials and products for the eco-construction in the building and civil engineering field (Cenicenta), funded by the Innovation Galician Agency, Galician Government (Xunta de Galicia), FEDER 2014-2020, Call 2016.

#### References

- [1] S. Peña, R.E. de E. (REE), 14 de diciembre de 2019: ¿El principio del fin del carbón?, (n.d.). <https://red2030.com/2019-fin-carbon/>.
- [2] EUROCOAL, EUROCOAL Statistics, (2020). <https://euracoal.eu/info/euracoal-eu-statistics/>.
- [3] H.K. Kim, H.K. Lee, Coal bottom ash in field of civil engineering: A review of advanced applications and environmental considerations, *KSCSE J. Civ. Eng.* 19 (2015) 1802–1818, <https://doi.org/10.1007/s12205-015-0282-7>.
- [4] K. Muthusamy, M.H. Rasid, G.A. Johkio, A. Mokhtar, Albshir Budiea, M.W. Hussin, J. Mirza, Coal bottom ash as sand replacement in concrete: A review, *Constr. Build. Mater.* 236 (2020), <https://doi.org/10.1016/j.conbuildmat.2019.117507>.
- [5] I.M. Nikbin, R.R. Saman, H. Allahyari, M. Damadi, A comprehensive analytical study on the mechanical properties of concrete containing waste bottom ash as natural aggregate replacement, *Constr. Build. Mater.* 121 (2016) 746–759, <https://doi.org/10.1016/j.conbuildmat.2016.06.078>.
- [6] N. Singh, M. Mithulraj, S. Arya, Influence of coal bottom ash as fine aggregates replacement on various properties of concretes: A review, *Resour. Conserv. Recycl.* 138 (2018) 257–271, <https://doi.org/10.1016/j.resconrec.2018.07.025>.
- [7] G. Sua-lam, N. Makul, Utilization of coal- and biomass-fired ash in the production of self-consolidating concrete: A literature review, *J. Clean. Prod.* 100 (2015) 59–76, <https://doi.org/10.1016/j.jclepro.2015.03.038>.
- [8] R. Rodríguez-Álvarez, S. Seara-Paz, B. González-Fontebao, F. Martínez-Abella, Use of granular coal combustion products as aggregates in structural concrete: Effects on properties and recommendations regarding mix design, *Constr. Build. Mater.* (2020), <https://doi.org/10.1016/j.conbuildmat.2020.121690>.
- [9] P. Torikittikul, T. Nochaiya, W. Wongkeo, Utilization of coal bottom ash to improve thermal insulation of construction material, *J. Mater. Cycles Waste Manag.* (2015), <https://doi.org/10.1007/s10163-015-0419-2>.
- [10] E. Baite, A. Messan, K. Hannawi, F. Tsohnang, W. Prince, Physical and transfer properties of mortar containing coal bottom ash aggregates from Tefereyre (Niger), *Constr. Build. Mater.* 125 (2016) 919–926, <https://doi.org/10.1016/j.conbuildmat.2016.08.117>.
- [11] H.K. Kim, J.H. Jeon, H.K. Lee, Flow, water absorption, and mechanical characteristics of normal- and high-strength mortar incorporating fine bottom ash aggregates, *Constr. Build. Mater.* 26 (2012) 249–256, <https://doi.org/10.1016/j.conbuildmat.2011.06.019>.
- [12] H.K. Kim, H.K. Lee, Use of power plant bottom ash as fine and coarse aggregates in high-strength concrete, *Constr. Build. Mater.* 25 (2011) 1115–1122, <https://doi.org/10.1016/j.conbuildmat.2010.06.065>.
- [13] S.S.G. Hashemi, H. Bin Mahmud, J.N.Y. Djobo, C.G. Tan, B.C. Ang, N. Ranjbar, Microstructural characterization and mechanical properties of bottom ash mortar, *J. Cle.* 2018-Sept (2018) 797–804.
- [14] L.B. Andrade, J.C. Rocha, M. Cheriaf, Evaluation of concrete incorporating bottom ash as a natural aggregates replacement, *Waste Manag.* 27 (2007) 1190–1199, <https://doi.org/10.1016/j.wasman.2006.07.020>.
- [15] L.B. Andrade, J.C. Rocha, M. Cheriaf, Influence of coal bottom ash as fine aggregate on fresh properties of concrete, *Constr. Build. Mater.* 23 (2009) 609–614, <https://doi.org/10.1016/j.conbuildmat.2008.05.003>.
- [16] M. Singh, R. Siddique, K. Ait-Mokhtar, R. Belarbi, Durability properties of concrete made with high volumes of low-calcium coal bottom ash as a replacement of two types of sand, *J. Mater. Civ. Eng.* 28 (2016) 1–9, [https://doi.org/10.1061/\(ASCE\)MT.1943-5533.0001464](https://doi.org/10.1061/(ASCE)MT.1943-5533.0001464).
- [17] M. Rafiezonooz, M.R. Salim, J. Mirza, M.W. Hussin, R. Salmiati, E. Khankhaje Khan, Toxicity characteristics and durability of concrete containing coal ash as substitute for cement and river sand, *Constr. Build. Mater.* 143 (2017) 234–246, <https://doi.org/10.1016/j.conbuildmat.2017.03.151>.
- [18] B. Zhang, C.S. Poon, Use of Furnace Bottom Ash for producing lightweight aggregate concrete with thermal insulation properties, *J. Clean. Prod.* 99 (2015) 94–100, <https://doi.org/10.1016/j.jclepro.2015.03.007>.
- [19] N. Ghafouri, J. Bucholc, Properties of high-calcium dry bottom ash concrete, *ACI Mater. J.* 94 (1997) 90–101.
- [20] R. Raju, M.M. Paul, K.a. Aboobacker, Strength Performance of Concrete Using Bottom Ash As Fine, *Int. J. Res. Eng. Technol.* 2 (2014) 111–122.
- [21] R. Siddique, Compressive strength, water absorption, sorptivity, abrasion resistance and permeability of self-compacting concrete containing coal bottom ash, *Constr. Build. Mater.* 47 (2013) 1444–1450, <https://doi.org/10.1016/j.conbuildmat.2013.06.081>.
- [22] L.B. Andrade, J.C. Rocha, M. Cheriaf, Aspects of moisture kinetics of coal bottom ash in concrete, *Cem. Concr. Res.* 37 (2007) 231–241, <https://doi.org/10.1016/j.cemconres.2006.11.001>.
- [23] M. Singh, R. Siddique, Compressive strength, drying shrinkage and chemical resistance of concrete incorporating coal bottom ash as partial or total replacement of sand, *Constr. Build. Mater.* 68 (2014) 39–48, <https://doi.org/10.1016/j.conbuildmat.2014.06.034>.
- [24] M. Singh, R. Siddique, Strength properties and micro-structural properties of concrete containing coal bottom ash as partial replacement of fine aggregate, *Constr. Build. Mater.* 50 (2014) 246–256, <https://doi.org/10.1016/j.conbuildmat.2013.09.026>.
- [25] M. Singh, R. Siddique, Properties of concrete containing high volumes of coal bottom ash as fine aggregate, *J. Clean. Prod.* 91 (2015) 269–278, <https://doi.org/10.1016/j.jclepro.2014.12.026>.

- [26] M. Singh, R. Siddique, Effect of coal bottom ash as partial replacement of sand on workability and strength properties of concrete, *J. Clean. Prod.* 112 (2016) 620–630, <https://doi.org/10.1016/j.jclepro.2015.08.001>.
- [27] I. Yüksel, T. Bilir, Ö. Özkan, Durability of concrete incorporating non-ground blast furnace slag and bottom ash as fine aggregate, *Build. Environ.* 42 (2007) 2651–2659, <https://doi.org/10.1016/j.buildenv.2006.07.003>.
- [28] M.P. Kadam, D. Patil, Effect of coal bottom ash as sand replacement on the properties of concrete with different w/c ratio, *Int. J. Adv. Technol. Civ. Eng. ISSN.* (2013) 2231–5721, <https://doi.org/10.12691/ajcea-2-5-2>.
- [29] S.U. Shin, S. Kumar, M. Mohanty, V. Puri, K. Hsiao, Development and field demonstration of air-entrained concrete composites using Illinois PCC bottom ash, (2006).
- [30] R. Kasemchaisiri, S. Tangtermsirikul, Properties of self-compacting concrete incorporating bottom ash as a partial replacement of fine aggregate, *ScienceAsia.* 34 (2008) 87–95, <https://doi.org/10.2306/scienceasia1513-1874.2008.34.087>.
- [31] N. Ghafoori, Y. Cai, Laboratory-Made RCC containing Dry Bottom Ash: Part I—Mechanical Properties, *ACI Mater. J.* 95 (1998) 121–130, <https://doi.org/10.14359/357>.
- [32] N. Ghafoori, Y. Cai, Laboratory-made roller compacted concretes containing dry bottom ash: Part II - Long-term durability, *ACI Mater. J.* 95 (1998) 244–251, <https://doi.org/10.14359/368>.
- [33] G.M. Kim, J.G. Jang, H.R. Khalid, H.K. Lee, Water purification characteristics of pervious concrete fabricated with CSA cement and bottom ash aggregates, *Constr. Build. Mater.* 136 (2017) 1–8, <https://doi.org/10.1016/j.conbuildmat.2017.01.020>.
- [34] S.B. Park, Y. Il Jang, J. Lee, B.J. Lee, An experimental study on the hazard assessment and mechanical properties of porous concrete utilizing coal bottom ash coarse aggregate in Korea, *J. Hazard. Mater.* 166 (2009) 348–355, <https://doi.org/10.1016/j.jhazmat.2008.11.054>.
- [35] C. Nghopok, V. Sata, T. Satiennam, P. Klungboonkrong, P. Chindaprasit, Mechanical properties, thermal conductivity, and sound absorption of pervious concrete containing recycled concrete and bottom ash aggregates, *KSCCE J. Civ. Eng.* 22 (2018) 1369–1376, <https://doi.org/10.1007/s12205-017-0144-6>.
- [36] K. Antoni, M. Klarens, L. Al Indranata, D. Hardjito Jamali, The use of bottom ash for replacing fine aggregate in concrete paving blocks, *MATEC Web Conf.* 138 (2017), <https://doi.org/10.1051/mateconf/201713801005>.
- [37] R. Karolina, N. Bahri Syahrizal, Optimization of fly ash and bottom ash substitution against paving block manufacture according to SNI 03–0691–1996, *IOP Conf. Ser. Mater. Sci. Eng.* 309 (2018), <https://doi.org/10.1088/1757-899X/309/1/012134>.
- [38] A.A. Hosin, B. Kroeger, S.-C. Yen, K. Hsiao, S.S. Marikunte, D. Olive, Fiber reinforced coal combustion products concrete, *Southern Illinois University Carbondale*, 2007. doi:10.2320/materia.46.171.
- [39] C. García Arenas, M. Marrero, C. Leiva, J. Solís-Guzmán, L.F. Vilches Arenas, High fire resistance in blocks containing coal combustion fly ashes and bottom ash, *Waste Manag.* 31 (2011) 1783–1789, <https://doi.org/10.1016/j.wasman.2011.03.017>.
- [40] H. Hansika, A. Nanayakkara, Investigation on Properties of Cellular Lightweight Concrete Blocks with Bottom Ash, *MERCon, Proceedings, 5th Int Multidiscip. Moratuwa Eng. Res. Conf.* 2019 (2019) 424–429, <https://doi.org/10.1109/MERCon.2019.8818756>.
- [41] A.K. Mandal, O.P. Sinha, Production of thermal insulation blocks from bottom ash of fluidized bed combustion system, *Waste Manag. Res.* 35 (2017) 810–819, <https://doi.org/10.1177/0734242X17707575>.
- [42] A. Ghosh, A. Ghosh, S. Neogi, Reuse of fly ash and bottom ash in mortars with improved thermal conductivity performance for buildings, *Heliyon.* 4 (2018), <https://doi.org/10.1016/j.heliyon.2018.e00934>.
- [43] S. Naganathan, S. Jamali, S. Silvadanan, T.Y. Chung, M.F. Nicolasselvam, Use of Bottom Ash and Fly Ash in Masonry Mortar, 01 (2016) 52–57.
- [44] P. Ramadoss, T. Sundararajan, Utilization of Lignite-Based Bottom Ash as Partial Replacement of Fine Aggregate in Masonry Mortar, *Arab. J. Sci. Eng.* 39 (2014) 737–745, <https://doi.org/10.1007/s13369-013-0703-1>.
- [45] J.Y. Yoon, J.Y. Lee, J.H. Kim, Use of raw-state bottom ash for aggregates in construction materials, *J. Mater. Cycles Waste Manag.* 21 (2019) 838–849, <https://doi.org/10.1007/s10163-019-00841-5>.
- [46] J.H.J. Kim, Y. Mook Lim, J.P. Won, H.G. Park, Fire resistant behavior of newly developed bottom-ash-based cementitious coating applied concrete tunnel lining under RABT fire loading, *Constr. Build. Mater.* 24 (2010) 1984–1994, <https://doi.org/10.1016/j.conbuildmat.2010.04.001>.
- [47] P. Onprom, K. Chaimoon, R. Cheerarat, Influence of Bottom Ash Replacements as Fine Aggregate on the Property of Cellular Concrete with Various Foam Contents, *Adv. Mater. Sci. Eng.* 2015 (2015), <https://doi.org/10.1155/2015/381704>.
- [48] M.O. Carmona, J.G. Paules, J.C.S. Catalán, L.F. Pousa, Reciclado de escorias de fondo de central térmica para su uso como áridos en la elaboración de componentes prefabricados de hormigón Recycling power plant slag for use as aggregate in precast concrete components, 60 (2010) 99–113. doi:10.3989/mc.2010.52109.
- [49] C. Arenas, C. Leiva, L.F. Vilches, H. Cifuentes, Use of co-combustion bottom ash to design an acoustic absorbing material for highway noise barriers, *Waste Manag.* 33 (2013) 2316–2321, <https://doi.org/10.1016/j.wasman.2013.07.008>.
- [50] E. López-López, Á. Vega-Zamanillo, M.Á. Calzada-Pérez, M.Á. Taborga-Sedano, Use of bottom ash from thermal power plant and lime as filler in bituminous mixtures, *Mater. Construcción.* 65 (2015).
- [51] American Coal Ash Association (ACAA), ACAA 2018 CCP Survey Results and Production & Use, 2020. <https://www.aaa-usa.org/publications/productionuserreports.aspx>.
- [52] J.Y. Park, *Wastes as Resources: The Case of Coal Combustion By-products in the United States*, Yate University (2012).
- [53] A.S. Cadarsa, I. Auckburally, Use of Unprocessed Coal Bottom Ash as Partial Fine Aggregate Replacement in Concrete, 20 (2014) 62–84.
- [54] D. Walach, Impact of separated bottom ashes on the parameters of concrete mix and hardened concrete, *E3S Web Conf.* 10 (2016), <https://doi.org/10.1051/e3sconf/20161000099>.
- [55] M.H.W. Ibrahim, A.F. Hamzah, N. Jamaluddin, P.J. Ramadhansyah, A.M. Fadzil, Split Tensile Strength on Self-compacting Concrete Containing Coal Bottom Ash, *Procedia - Soc. Behav. Sci.* 195 (2015) 2280–2289, <https://doi.org/10.1016/j.sbspro.2015.06.317>.
- [56] Concrete Block Association, Aggregate Block Sustainability, (2017). <https://www.cba-blocks.org.uk/wp-content/uploads/2018/03/CBA-2pp-Aggregate-Block-datasheet-rnd2.pdf>.
- [57] ANDECE, *Industria Prefabricado Hormigón, Muros de bloques y ladrillos de hormigón*, Ind. Prefabr. Del Hormig. (2019).
- [58] R.V. Silva, J. De Brito, R.K. Dhir, Performance of cementitious renderings and masonry mortars containing recycled aggregates from construction and demolition wastes, *Constr. Build. Mater.* 105 (2016) 400–415, <https://doi.org/10.1016/j.conbuildmat.2015.12.171>.
- [59] I. Vegas, I. Azkarate, A. Juarrero, M. Frías, Diseño y prestaciones de morteros de albañilería elaborados con áridos reciclados procedentes de escombros de hormigón, *Mater. Constr.* 59 (2009) 5–18, <https://doi.org/10.3989/mc.2009.44207>.
- [60] A.B. De Melo, E.P. Silva, Bloques de hormigón ligero con áridos reciclados de EVA: Una contribución a la eficiencia térmica de paredes exteriores de edificios, *Mater. Constr.* 63 (2013) 479–495, <https://doi.org/10.3989/mc.2013.05912>.
- [61] J. Faustino, E. Silva, J. Pinto, E. Soares, V.M.C.F. Cunha, S. Soares, Lightweight concrete masonry units based on processed granulate of corn cob as aggregate, *Mater. Constr.* 65 (2015), <https://doi.org/10.3989/mc.2015.04514>.
- [62] Z. Sánchez-Roldán, M. Martín-Morales, I. Valverde-Palacios, I. Valverde-Espinosa, M. Zamorano, Study of potential advantages of pre-soaking on the properties of pre-cast concrete made with recycled coarse aggregate, *Mater. Constr.* 66 (2016), <https://doi.org/10.3989/mc.2016.01715>.
- [63] National Concrete Masonry Association, What is the difference between a “cinder block” and a “concrete block”?, (2014) 1–3. [http://ncma-br.org/pdfs/masterlibrary/FAQ\\_20-14\\_Concrete\\_Block\\_vs\\_Cinder\\_Block.pdf](http://ncma-br.org/pdfs/masterlibrary/FAQ_20-14_Concrete_Block_vs_Cinder_Block.pdf).
- [64] American Society for Testing and Materials (ASTM), ASTM C331-17: Standard Specification for Lightweight Aggregates for Concrete Masonry Units, (2017).
- [65] AENOR, UNE-EN, 933-1 Tests for geometrical properties of aggregates. Part 1: Determination of particle size distribution, Sieving method. (2012).
- [66] Ministerio de fomento, Gobierno de España., EHE Instrucción Española del Hormigón Estructural, (2008).
- [67] AENOR, UNE 146301 Aggregates. Fineness modulus of the fine aggregate., (2002).
- [68] AENOR, UNE-EN, 933-8 Tests for geometrical properties of aggregates. Part 8: Assessment of fines, Sand Equivalent Test (2015).
- [69] N.Y.S.D. of T.M. Bureau, NY 703-19 E Moisture content of lightweight fine aggregate, (2008) 1–4.
- [70] AENOR, UNE 146404 Aggregates for concrete. Determination of the coefficient of friability of the sands., (2018).
- [71] AENOR, UNE 103204 Organic matter content of a soil by the potassium permanganate method., (2019).
- [72] AENOR, UNE 146508 Test for aggregates. Determination of the alkali-silica and alkali-silicate potential reactivity of aggregates. Accelerated mortar bar test., (2018).
- [73] RC-16, Real Decreto 256/2016, de 10 de junio, por el que se aprueba la Instrucción para la recepción de cementos (RC-16), (2016). doi:BOE-A-2012-5403.
- [74] C. Martínez-García, B. González-Fontebosa, D. Carro-López, F. Martínez-Abella, Design and properties of cement coating with mussel shell fine aggregate, *Constr. Build. Mater.* 215 (2019) 494–507, <https://doi.org/10.1016/j.conbuildmat.2019.04.211>.
- [75] AENOR, UNE 127771-3 Requirements and delivery and reception conditions of aggregate concrete masonry units (dense and light-weight aggregates). National complement to the standard UNE-EN 771-3., (2008).
- [76] S.L. Prefhorisa Outeiro, *Fichas técnicas, Declaración de prestaciones (2005)*.
- [77] AENOR, UNE-EN 771-3 Specification for masonry units. Part 3: Aggregate concrete masonry units (Dense and lightweight aggregates), (2011).
- [78] AENOR, UNE-EN 1015-3 Methods of test for mortar for masonry. Part 3: Determination of consistence of fresh mortar (by flow table), (2000) 12.
- [79] AENOR, UNE-EN 1015-4 Methods of test for mortar for masonry. Part 4: Determination of consistence of fresh mortar (by plunger penetration), (1999).
- [80] AENOR, UNE-EN 480-4 Admixtures for concrete, mortar and grout. Test methods. Part 4: Determination of bleeding of concrete, (2006).
- [81] AENOR, UNE-EN 1015-9 Methods of test for mortar for masonry. Part 9: Determination of workable life and correction time of fresh mortar, (2000).
- [82] AENOR, UNE-EN 1015-6:2000 Methods of test for mortar for masonry. Part 6: Determination of bulk density of fresh mortar, (1999) 12.
- [83] AENOR, UNE 83980 Concrete durability. Test methods. Determination of the water absorption, density and accessible porosity for water in concrete, (2014).
- [84] AENOR, UNE-EN 1015-7 Methods of test for mortar for masonry. Part 7: Determination of air content of fresh mortar, (1999).



- [85] AENOR, UNE-EN 1015-11 Methods of test for mortar for masonry. Part 11: Determination of flexural and compressive strength of hardened mortar, (2000).
- [86] AENOR, UN E-EN 12390-3 Testing h ardened concrete. Part 3: Compressive strength of test specimens, (2009).
- [87] AENOR, UN E-EN 12390-6 Testing h ardened concrete. Part 6: Tensile splitting strength of test specimens., (2010).
- [88] AENOR, UNE-EN 772-1:2011+A1 Methods of test for masonry units. Part 1: Determination of compressive strength., (2016).
- [89] AENOR, UNE-EN 1015-18 Methods of test for mortar for masonry. Part 18: Determination of water absorption coefficient due to capillary action of hardened mortar, (2003).
- [90] AENOR, UNE 83982 Concrete durability. Test methods. Determination of the capillar suction in hardened concrete. Fagerlund method, (2008).
- [91] AENOR, UN E-EN 772-11 Methods of test for masonry units. Part 11: Determination of water absorption of aggregate concrete, autoclaved aerated concrete, manufactured stone and natural stone masonry y units due to capillary action and the initial rate of water abs, (2011).
- [92] AENOR, UNE-EN 12617-4 Products and systems for the protection and repair of concrete structures. Test methods. Part 4: Determination of shrinkage and expansion, (2002).
- [93] ASTM, ASTM C1761: Lightweight Aggregate for Internal Curing of Concrete, (2015). doi:10.1520/C1761.